Proceedings of the ASME 2011 International Design Engineering Technical Conferences & Computers and Information in Engineering Conference
IDETC/CIE 2011
August 29-31, 2011, Washington, DC, USA

DETC2011/CIE-47740

ON THE CONSTITUTIVE RESPONSE CHARACTERIZATION FOR COMPOSITE MATERIALS VIA DATA-DRIVEN DESIGN OPTIMIZATION

John G. Michopoulos
Computational Multiphysics Systems Lab.
Center of Computational Material Science
Naval Research Laboratory
Washington, DC, USA

John G. Hermanson
Wood Based Materials & Structures
Forest Products Laboratory
USDA Forest Service
Madison, WI, USA

Athanasios Iliopoulos
Science Applications Int. Corp.
resident at Naval Research Laboratory
Washington DC 20375, USA

Samuel Lambrakos
Computational Multiphysics Systems Lab.
Center of Computational Material Science
Naval Research Laboratory
Washington, DC, USA

Tomonari Furukawa
Computational Multiphysics Lab.
Dpt. of Mechanical Engineering
Virginia Polytechnic Institute and State University
Danville, VA, USA

ABSTRACT

In the present paper we focus on demonstrating the use of design optimization for the constitutive characterization of anisotropic material systems such as polymer matrix composites, with or without damage. All approaches are based on the availability of experimental data originating from mechatronic material testing systems that can expose specimens to multidimensional loading paths and can automate the acquisition of data representing the excitation and response behavior of the specimens involved. Material characterization is achieved by minimizing the difference between experimentally measured and analytically computed system responses as described by strain fields and surface strain energy densities. A one dimensional model is presented first to elucidate the design optimization for the general non-linear constitutive response. Small and large strain formulations based on strain energy density decompositions are developed and utilized for determining the constitutive behavior of composite materials. Examples based on both synthetic and actual data demonstrate the successful application of design optimization for constitutive characterization.

INTRODUCTION

Design optimization as a topic of research relative to engineering applications and product development has been popular within the context of optimal shape determination but not as popular within the context of material characterization. In an attempt to fill this gap, the main objective of the present paper is to describe design optimization efforts in the less popular application area of the data-driven constitutive characterization of anisotropic material systems.

Composite materials are clearly the most widely used anisotropic materials for various application areas [1, 2]. Their constitutive characterization has been an important topic of interest for structural design, material certification and qualification practitioners. Such characterization has been traditionally achieved through conventional uniaxial tests and used for deter-

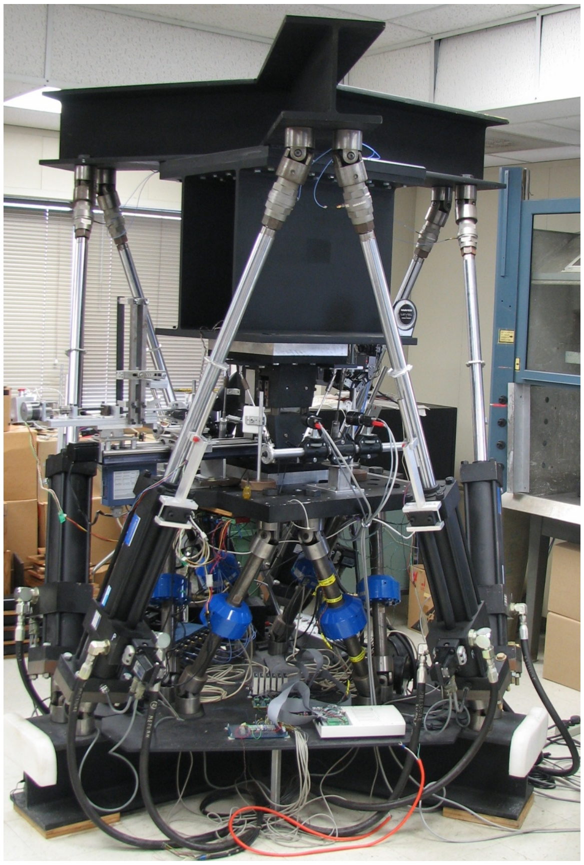

FIGURE 1: NRL66.3: Most recent 6-DoF mechatronically automated system for the multi-axial testing of composite materials

mining elastic properties. Typically, extraction of these properties, involve uniaxial tests conducted with specimens mounted on uniaxial testing machines, where the major orthotropic axis of any given specimen is angled relative to the loading direction. In addition, specimens are designed such that a homogeneous state of strain is developed over a well defined area, which is for the purpose of measuring kinematic quantities [3, 4]. Consequently, the use of uniaxial testing machines imposes requirements of using multiple specimens, griping fixtures and multiple experiments. The requirement of a homogeneous state of strain frequently imposes restrictions on the sizes and shapes of specimens to be tested. It follows that these requirements result in increased cost and time, and consequently to inefficient characterization processes.

To address these issues and to extend characterization to non-linear regimes, multi-degree of freedom automated mechatronic testing machines, which are capable of loading specimens multiaxially in conjunction with energy-based inverse characterization methodologies, were introduced at the Naval Research Laboratory (NRL) [5–7]. This introduction was the first of its kind and has continued through the present [8–10]. The most recent prototype of these machines, which is currently under verification, is shown in Fig. 1.

The energy-based approach associated with mechatronic testing, although it enables multiaxial loading and inhomogeneous states of strain, still requires multiple specimens. It is significant to state however, that these specimens are tested in a automated manner with high throughput of specimens per hour, which have reached values of 30 specimens per hour.

The recent development of flexible full-field displacement and strain measurements methods has afforded the opportunity of alternative characterization methodologies [11–14]. Full-field optical techniques, such as Moire and Speckle Interferometry, Digital Image Correlation (DIC), and Meshless Random Grid Method (MRGM), which measure displacement and strain fields during mechanical tests, have been used mostly for elastic characterization of various materials [14–17]. The resulting measurements are used for identification of constitutive model constants, via the solution of an appropriately formed inverse problem, with the help of various computational techniques.

Arguably, the most popular methodology is the mixed numerical/experimental method that identifies the material's elastic constants by minimizing an objective function formed by the difference between the full-experimental measurements and the corresponding analytical model predictions via an optimization method [5–10, 14, 17–19]. However, the repetitive finite element analysis (FEA) required for each iteration of the optimization process, makes the computation considerably costly [20]. Alternatively, the so-called virtual field method was developed [20–22] to identify material parameters by finding virtual fields and inversely solving for parameters by substitution of full-field/surface measurements. That is to say, the virtual field method effectively characterizes materials without finite element analysis, provided that appropriate virtual fields are derivable.

Our focus in the present work is to describe recent efforts concerning design optimization methodologies for constitutive material characterization. Our approaches are based mostly on energy conservation arguments, and they can be classified according to computational cost in relation to the iterative use of FEA or not. It is important to clarify that digitally acquired images are processed by software [23] that implements the MRGM [14, 24–28] and is used to extract the full-field displacement and strain field measurements as well as the boundary displacements required for material characterization. Reaction forces and redundant boundary displacement data are acquired from displacement and force sensors integrated with NRL's multiaxial loader called NRL66.3 [29]. In an effort to address the computational cost of the FEA-in-the-loop approaches, the authors have initiated a dissipated and total strain energy density determination approach that has recently been extended to a framework that is derived from the total potential energy and the energy conservation, which can be applied directly with full field strain measurement for characterization [30–35].

Two techniques, built upon this framework, have been proposed to identify elastic constants and to develop non-parametric constitutive models of anisotropic materials.

The first identification technique estimates the elastic constants for every set of measurements by equating the variation of the external work, derived from the boundary displacement/force measurements, with that of the induced strain energy, derived from the full-field strain measurements, and stochastically correcting the estimation using Kalman filter [35]. This technique has been proven to identify the elastic constants of anisotropic materials even under the presence of considerable noise in the measurements.

The second technique develops non-parametric representations of constitutive models using artificial neural networks [36]. When we first explored this approach in the early nineties [37], it was established that the computational performance of the approach, as it was implemented on the Aspirin/MIGRAINES neural net simulator framework [38], was not practical for the amounts of data generated by NRL's multidimensional testing machines. Subsequently, we have applied it on many other material characterization applications [39–43]. We have established how improvements in the evolving computational technologies have impacted positively the feasibility of more demanding applications. In that both ANN implementations and full field measurement techniques have matured, we have decided to apply ANN technologies for material characterization [32]. The error between the energy quantities is used to develop the neural network constitutive model, unlike the conventional techniques where stress data are required for the modeling [44–47]. This technique allows the nonlinear constitutive relations to be modeled comprehensively without the limitations imposed by the parametric expressions of the conventional material models. Accordingly, this technique has been applied to model the damage behavior of composite materials [48, 49].

In order to maintain reasonable scope this paper considers only methodologies that require FEA-in-the-loop because of the simplicity of their implementation and exhaustive capability to determine the material parameters. The consideration of other methodologies is more appropriate for future comparative studies.

In the section that follows we present the case of determining the properties of the one-dimensional non-linear system. This is done mainly for instructive purposes, which bare relevance to subtleties of subsequent formulations presented. Next, we present a small strain formulation (SSF) of the general strain energy density approach followed by a finite strain formulation (FSF), which is for the case of linear and non-linear constitutive behavior of composite materials with or without damage. The paper continuous with a numerical application of design optimization implementations based on these two formulations, which are in turn based on both synthetic and actual data. Finally conclusions are presented.

THE CASE OF ONE DIMENSIONAL MATERIAL SYSTEM

To introduce design optimization for material characterization in a fashion of increasing complexity we consider first a one-dimensional system that possesses both linear recoverable and non-linear irrecoverable responses. The template approach that we will employ first for this simple case and then for more realistic cases is that of defining a Strain Energy Density function (SED) that governs the material behavior and indirectly contains the actual constitutive behavior.

$$\begin{aligned} U_{1D} &= U_{1D}^R(C,\varepsilon) + U_{1D}^I(C,\beta_i;\varepsilon) = \\ &= \left[\frac{1}{2}C\varepsilon^2\right]_{1D}^R + \left[D(\beta_i;\varepsilon)\frac{1}{2}C\varepsilon^2\right]_{1D}^I \end{aligned} \tag{1}$$

where $U_{1D}^R(C,\varepsilon), U_{1D}^I(C,\beta_i;\varepsilon)$ are the recoverable (elastic) SED and the irrecoverable (inelastic or dissipated) SED, respectively. The quantities $C, \beta_i, D(C,\beta_i;\varepsilon)$are the stiffness constant (modulus of elasticity), the constants participating in the dissipated energy coefficient function, and the dissipated energy density coefficient function, itself, respectively. Equation 1 implies that the irrecoverable or dissipated strain energy density (DSED) has been constructed to be a multiplicative decomposition with weighting $D(\beta_i;\varepsilon)$ for the recoverable SED according to:

$$U_{1D}^I(C,\beta_i;\varepsilon) = D(\beta_i;\varepsilon)U_{1D}^R(C,\varepsilon) \tag{2}$$

The functional form of $D(\beta_i;\varepsilon)$ should be one that ensures energy dissipation in a manner that yields a softening of nonlinear stress-strain constitutive response. There are many forms that have this property, based on transcendental functions, which have been used in the past [50]. Here we employ a functional form that can be expanded in a Taylor series. This functional form provides for a polynomial representation that is necessary condition for algebraic reducibility and is therefore convenient for the application of transformations. This form of the DSED, which is initially negligible and then monotonically increasing, can be represented by the following physically consistent choice of $D(\beta_i;\varepsilon)$:

$$D(\beta_i;\varepsilon) = D(m,\varepsilon_f;\varepsilon) = 1 - e^{-\frac{1}{me}\left(\frac{\varepsilon}{\varepsilon_f}\right)^m} \tag{3}$$

where $\beta_1 = m, \beta_2 = \varepsilon_f$ are the two material parameters controlling the dissipative nature of the material behavior. The exponent

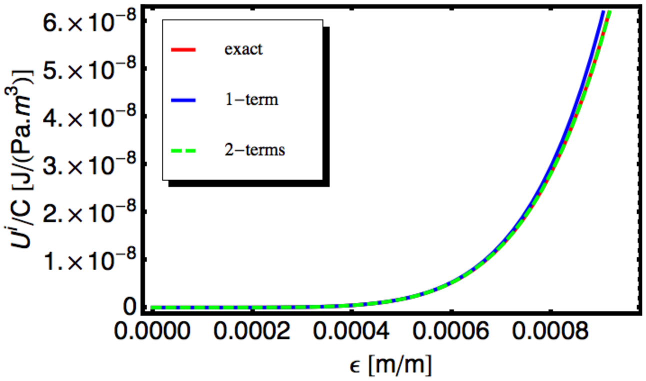

FIGURE 2: Difference of 1- and 2-term approximations of normalized irrecoverable or dissipated energy density as a function of strain relative to the exact model

m controls the level of non-linearity involved in the model and $\varepsilon_f$expresses the level of failure strain. The series expansion of $\bar{D}(m, \varepsilon_f; \varepsilon)$ defined by Eq. 3 yields

$$\bar{D}(m, \varepsilon_f; \varepsilon) = \sum_{k=1}^{n} \frac{(-1)^k}{k!} \left(\frac{1}{me}\right)^k \left(\frac{\varepsilon}{\varepsilon_f}\right)^{mk}. \tag{4}$$

Given Eq. 4 and 1, it follows that Eq. 2 may be expressed by

$$U_{1D}^I(C, \beta_i; \varepsilon) = \frac{1}{2} C \sum_{k=1}^{n} \frac{(-1)^k}{k!} \left(\frac{1}{me}\right)^k \left(\frac{\varepsilon}{\varepsilon_f}\right)^{mk} \varepsilon^2 \tag{5}$$

A plot of the function defined by Eq. 5, normalized by the Elastic constant C, is presented in Fig. 2 for $m = 4$ and $\varepsilon_f = 0.0008$. Referring to Fig. 2 it can be seen that for more than two terms the series expression gives essentially identical results to those of the exact evaluation of DSED. It is interesting to note that the single term expression is also in good agreement with the exact form. Therefore, we can truncate all but the first term in Eq. 5 to obtain:

$$U_{1D}^I(C, \beta_i; \varepsilon) = -\frac{1}{2} C \left(\frac{1}{me}\right) \left(\frac{\varepsilon}{\varepsilon_f}\right)^m \varepsilon^2 \tag{6}$$

It follows then that, Eq. 1 can be expressed

$$\begin{aligned} U_{1D} &= U_{1D}^R(C, \varepsilon) + U_{1D}^I(C, \beta_i; \varepsilon) = \\ &= \frac{1}{2} C \varepsilon^2 - \frac{1}{2} C \left(\frac{1}{me}\right) \left(\frac{\varepsilon}{\varepsilon_f}\right)^m \varepsilon^2 \end{aligned} \tag{7}$$

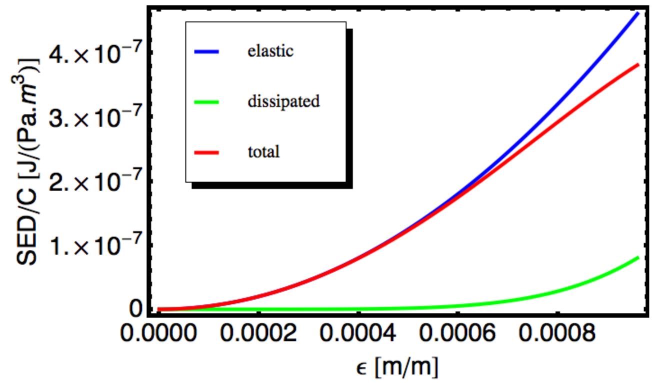

(a) Distribution of elastic, dissipated (or irrecoverable) and total SEDs for one dimensional case

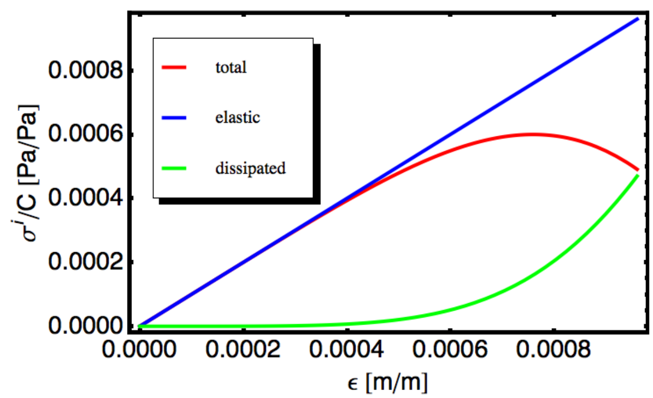

(b) Stress distributions as a function of strain

FIGURE 3: SED and corresponding stress distribution

For the case of generalized hyperelasticity as special case of which is elasticity, the corresponding constitutive law will be given by

$$\begin{aligned} \sigma_{1D} &= \frac{\partial [U_{1D}^R(C, \varepsilon) + U_{1D}^I(C, \beta_i; \varepsilon)]}{\partial \varepsilon} = \\ &= \sigma_{1D}^R(C, \varepsilon) + \sigma_{1D}^I(C, \beta_i; \varepsilon) = \\ &= C\varepsilon - C \left(\frac{2+m}{2me}\right) \left(\frac{\varepsilon^{m+1}}{\varepsilon_f^m}\right) \end{aligned} \tag{8}$$

The resulting constitutive law contains the linear elastic part, as expected, but modified by a non-linear inelastic term. An indicative variation of total SED and its components (recoverable and irrecoverable SEDs), as described by Eq. 7 are shown in Fig. 3(a). Figure 3(b) shows the corresponding stress distribution defined by the constitutive law expressed by Eq. 8.

In the present formulation, the material parameters to be identified, or estimated based on experimental data, are the stiffness parameter and the two dissipated energy parameters C, m, ε_f.

The results of applying design optimization for determining these material parameters for 20 data points created synthetically by the material model defined Eq. 7 or 8 are shown in Table 1 for various methods.

These results indicate that Nelder-Mead and Differential evolution Methods are able to determine the properties exactly, while Simulated Annealing takes much longer and achieves less accurate parameter determinations.

COMPOSITE MATERIAL SYSTEM

For the general case of a composite material system we consider that a modified anisotropic hyperelastic strain energy density function can be constructed to encapsulate both the elastic and the inelastic responses of the material. However, certain classes of composite materials reach failure after small strains and some under large strains. For this reason we give two examples, one involving a small (infinitesimal) strain formulation (SSF) and another involving an finite (large) strain formulation (FSF).

Small Strain Formulation For the SSF we introduce a SED function that, in its most general form, can be represented as a scaled Taylor expansion of the Helmholtz free energy of a deformable body, which is in terms of small strain invariants of the form

$$
\begin{aligned}
U_{SSF}(I_1, I_2, I_3) = s_0 + s_{11}I_1 + \frac{1}{2}s_{12}I_1^2 + \frac{1}{3!}s_{13}I_1^3 + \\
+\frac{1}{4!}s_{14}I_1^4 + \ldots + s_{21}I_2 + \frac{1}{2}s_{22}I_2^2 + \frac{1}{3!}s_{23}I_2^3 + \\
+\frac{1}{4!}s_{24}I_2^4 + \ldots + \frac{1}{2}s_{13}I_3^2 + \frac{1}{3!}s_{13}I_3^3 + \frac{1}{4!}s_{14}I_3^4 + \\
\ldots + \frac{1}{2}s_{1121}I_1I_2 + \frac{1}{3!}s_{1221}I_1^2I_2 + \frac{1}{3!}s_{1122}I_1I_2^2 + \ldots \\
+\frac{1}{2}s_{1131}I_1I_3 + \frac{1}{3!}s_{1331}I_1^2I_3 + \frac{1}{3!}s_{1133}I_1I_3^2 + \ldots + \\
\frac{1}{4!}s_{1321}I_1^3I_2 + \frac{1}{4!}s_{1221}I_1^2I_2^2 + \frac{1}{4!}s_{1123}I_1I_2^3 + \ldots
\end{aligned}
\tag{9}
$$

where the invariants are defined by

$$
\begin{aligned}
I_1 &= tr(\varepsilon) = \varepsilon_{ii}, \\
I_2 &= \frac{1}{2}tr(\varepsilon^2) = \frac{1}{2}\varepsilon_{ij}\varepsilon_{ij}, \\
I_3 &= \frac{1}{2}tr(\varepsilon^3) = \frac{1}{3}\varepsilon_{ij}\varepsilon_{jk}\varepsilon_{ki}
\end{aligned}
\tag{10}
$$

The invariants are chosen to take advantage of a priori knowledge that the SED as a scalar quantity, must be invariant under frame reference translations and rotations. This follows in that the SED should be objective (i.e. independent of the observer's frame of reference).

An additive decomposition of this expression in terms of a recoverable and an irrecoverable SED can be expressed by

$$
U_{SSF} = U^R_{SSF}(S;\varepsilon_{ij}) + U^I_{SSF}(D;\varepsilon_{ij}). \tag{11}
$$

Clearly, all the second order monomials of strain components will be forming the recoverable part $U^R_{SSF}(S;\varepsilon_{ij})$ and the higher order monomials will be responsible for the irrecoverable part $U^I_{SSF}(D;\varepsilon_{ij})$. The resulting constitutive law is given by

$$
\begin{aligned}
\sigma_{ij} = \partial U_{SSF}/\partial\varepsilon_{ij} = \partial(U^R_{SSF}(S;\varepsilon_{ij}) + U^I_{SSF}(D;\varepsilon_{ij}))/\partial\varepsilon_{ij} = \\
= \frac{\partial U_{SSF}}{\partial I_1}\frac{\partial I_1}{\partial\varepsilon_{ij}} + \frac{\partial U_{SSF}}{\partial I_2}\frac{\partial I_2}{\partial\varepsilon_{ij}} + \frac{\partial U_{SSF}}{\partial I_3}\frac{\partial I_3}{\partial\varepsilon_{ij}}
\end{aligned}
\tag{12}
$$

A general expression which provides a strain dependent version of Eq. 11, is given by

$$
\begin{aligned}
U_{SSF} = U^R_{SSF}(S;\varepsilon_{ij}) + U^I_{SSF}(D;\varepsilon_{ij}) = \\
= \frac{1}{2}s_{ijkl}\varepsilon_{ij}\varepsilon_{kl} + d_{ijkl}(\varepsilon_{ij})\varepsilon_{ij}\varepsilon_{kl}
\end{aligned}
\tag{13}
$$

where s_{ijkl} are the components of the elastic stiffness tensor (Hooke's tensor) and $d_{ijkl}(\varepsilon_{ij})$ are strain-dependent damage functions, which fully define irrecoverable or dissipated strain energy density given by enforcing the dissipative nature of energy density. The quantity $d_{ijkl}(\varepsilon_{ij})$ can be defined in a manner analogous to that employed for the 1D system described above and is given by

$$
d_{ijkl}(\varepsilon_{ij}) = s_{ijkl}(1 - e^{(-\frac{\varepsilon_{ij}}{q_{ij}})^{p_{ij}}/(ep_{ij})}) \tag{14}
$$

TABLE 1: Design optimization results for a non-linear 1D material system

Method.	Objective Function	C [GPa]	m	ε_f
Target values	0.00	130.00	4.	0.0008
Nelder Mead	-0.0000116825	130.00	4.	0.0008
Differential Evolution	-0.00000429153	130.00	4.	0.0008
Simulated Annealing	134234	131.21	3.1	0.000856

As in the 1D case, we perform an equivalent series expansion and subsequently drop all terms except the first, in that it captures almost all of the dissipative behavior. Accordingly,

$$
\begin{aligned}
d_{ijkl}(\varepsilon_{ij}) &= s_{ijkl}\sum_{m=1}^{n}(-1)^m\left(\frac{1}{ep_{ij}}\right)^m\frac{\varepsilon_{ij}^{mp_{ij}}}{m!q_{ij}^{mp_{ij}}} = \\
&= s_{ijkl}\left(-\left(\frac{1}{ep_{ij}}\right)\frac{\varepsilon_{ij}^{p_{ij}}}{q_{ij}^{p_{ij}}}+\left(\frac{1}{ep_{ij}}\right)^2\frac{\varepsilon_{ij}^{2p_{ij}}}{2q_{ij}^{2p_{ij}}}-\cdots+\right) \simeq \\
&\simeq -s_{ijkl}\left(\frac{1}{ep_{ij}}\right)\frac{\varepsilon_{ij}^{p_{ij}}}{q_{ij}^{p_{ij}}}
\end{aligned} \tag{15}
$$

Thus the irrecoverable part of the energy in Eq. 11 becomes:

$$
\begin{aligned}
U_{SSF}^{I}(D;\varepsilon_{ij}) &= U_{SSF}^{I}(s_{ijkl},p_{ij},q_{ij};\varepsilon_{ij}) = \\
&= -s_{ijkl}\frac{1}{e(2+p_{ij})p_{ij}q_{ij}^{p_{ij}}}\varepsilon_{ij}^{1+p_{ij}}\varepsilon_{kl}
\end{aligned} \tag{16}
$$

Next, substituting Eq. 14 into Eq. 11 yields

$$
\begin{aligned}
U_{SSF} &= U_{SSF}^{R}(S;\varepsilon_{ij})+U_{SSF}^{I}(D;\varepsilon_{ij}) = \\
&= \frac{1}{2}s_{ijkl}\varepsilon_{ij}\varepsilon_{kl}-s_{ijkl}\frac{1}{e(2+p_{ij})p_{ij}q_{ij}^{p_{ij}}}\varepsilon_{ij}^{1+p_{ij}}\varepsilon_{kl}
\end{aligned} \tag{17}
$$

Applying Eq. 10 on Eq. 15, and employing Voight [3] notation for the case of a general orthotropic material, yields the constitutive relation

$$
\begin{bmatrix}\sigma_{xx}\\ \sigma_{yy}\\ \sigma_{zz}\\ \sigma_{xz}\\ \sigma_{yz}\\ \sigma_{xy}\end{bmatrix} = \begin{bmatrix} \breve{s_{xx}} & s_{xy} & s_{xz} & 0 & 0 & 0\\ s_{xy} & \breve{s_{yy}} & s_{yz} & 0 & 0 & 0\\ s_{xz} & s_{yz} & \breve{s_{zz}} & 0 & 0 & 0\\ 0 & 0 & 0 & \breve{s_{xz}} & 0 & 0\\ 0 & 0 & 0 & 0 & \breve{s_{yz}} & 0\\ 0 & 0 & 0 & 0 & 0 & \breve{s_{xy}}\end{bmatrix}\begin{bmatrix}\varepsilon_{xx}\\ \varepsilon_{yy}\\ \varepsilon_{zz}\\ \varepsilon_{xz}\\ \varepsilon_{yz}\\ \varepsilon_{xy}\end{bmatrix} \tag{18}
$$

where:

$$
\breve{s_{ij}} = s_{ij}\left(1-\bar{d_{ij}}\right) \tag{19}
$$

and

$$
\bar{d_{ij}} = \frac{1}{ep_{ij}q_{ij}^{p_{ij}}}\varepsilon_{ij}^{1+p_{ij}} \tag{20}
$$

All terms that are not shown in expression 18 are zero due to the orthotropic symmetry requirements. Therefore, the material parameters are the 9 elastic s_{ij} constants and $6\times 2 = 12$ damage constants p_{ij}, q_{ij} for a total of 21 parameters. Clearly, when the quantities $\bar{d_{ij}}$ do not depend on the strains and they are constants, Eq. 16 reduces to most of the continuous damage theories given by various investigators in the past [47,51–53]. For a transversely isotropic material the number of material parameters drops to 5+10=15 for a 3D state of strain and to 4+8=12 for a plane stress state.

Finite Strain Formulation The FSF can be written in a double additive decomposition manner. The first being the decomposition of the recoverable and irrecoverable SED, and the second being the decomposition between the volumetric (or dilatational) W_v and the distortional (or isochoric) W_d parts of the total SED. This decomposition is expressed by:

$$
\begin{aligned}
U_{SSF} = U^{R}_{SSF}(\alpha_i;J,\bar{C}) + U^{I}_{SSF}(\alpha_i,\beta_i;J,\bar{C}) = \\
= [W_v(J) + W_d(\bar{C},A\otimes A,B\otimes B)] - \\
-[d_v W_v(J) + d_d W_d(\bar{C},A\otimes A,B\otimes B)]
\end{aligned} \tag{21}
$$

where α_i, β_i are the elastic and inelastic material parameters of the system, respectively. A rearrangement of these decompositions, such as the volumetric vs. distortional decomposition, which appears on the highest expression level, leads to an expression introduced in [54], i.e.,

$$
U_{FSF} = (1-d_v)W_v(J) + (1-d_d)W_d(\bar{C},A\otimes A,B\otimes B), \tag{22}
$$

with the damage parameters $d_k \in [0,1], k \in [v,d]$ defined as

$$
d_k = d^{\infty}_{ka}\left[1 - e^{\left(-\frac{a_k(t)}{\eta_{ka}}\right)}\right] \tag{23}
$$

where $a_k(t) = \max_{s\in[0,t]} W^{o}_{k}(s)$ is the maximum energy component reached so far, and $d^{\infty}_{ka}, \eta_{ka}$ are two pairs of parameters controlling the energy dissipation characteristics of the two components of SED. In this formulation, $J = \det \underline{F}$ is the Deformation Gradient, $\bar{C} = \underline{F}^T \underline{F}$ is the right Cauchy Green (Green deformation) tensor, A, B are constitutive material directions in the undeformed configuration, and $A\otimes A, B\otimes B$ are microstructure structural tensors expressing fiber directions. Each of the two components of SED are defined as

$$
\begin{aligned}
W_v(J) = \frac{1}{d}(J-1)^2 W_d(\bar{C},A\otimes A,B\otimes B) = \\
= \sum_{i=1}^{3} a_i(\bar{I}_1-3)^i + \sum_{j=1}^{3} b_j(\bar{I}_2-3)^j + \sum_{k=1}^{6} c_k(\bar{I}_4-1)^k + \\
+ \sum_{l=2}^{6} d_l(\bar{I}_5-1)^l + \sum_{m=2}^{6} e_m(\bar{I}_6-1)^m + \sum_{n=2}^{6} f_n(\bar{I}_7-1)^n + \\
+ \sum_{o=2}^{6} g_o(\bar{I}_8-(A\cdot B)^2)^o
\end{aligned} \tag{24}
$$

where the strain invariants are defined as follows:

$$
\begin{aligned}
&\bar{I}_1 = tr\bar{C},\ \ \bar{I}_2 = \tfrac{1}{2}(tr^2\bar{C} - tr\bar{C}^2) \\
&\bar{I}_4 = A\cdot\bar{C}B,\ \ \bar{I}_5 = A\cdot\bar{C}^2 B \\
&\bar{I}_6 = B\cdot\bar{C}B,\ \ \bar{I}_7 = B\cdot\bar{C}^2 B,\ \ \bar{I}_8 = (A\cdot B)A\cdot\bar{C}B
\end{aligned} \tag{25}
$$

The corresponding constitutive behavior is given by the second Piola-Kirchhoff stress tensor according to [51]

$$
S = 2\frac{\partial U_{FSF}}{\partial C} \tag{26}
$$

or the usual Cauchy stress tensor according to

$$
\sigma_{FSF} = \frac{2}{J}F\cdot\frac{\partial U_{FSF}}{\partial C}\cdot F^T. \tag{27}
$$

Under the FSF formulation the material characterization problem involves determining the 36 coefficients (at most) of all monomials when the sums in the expression of distortional SED are expanded in Eq. 24, in addition to the compressibility constant d and the 4 parameters used in Eq. 23. It follows that potentially there can be a total of 41 material constants.

NUMERICAL RESULTS

For the purpose of demonstrating numerically the aforementioned concepts, the material selected for generating the necessary simulated experimental data is a typical laminate constructed from an epoxy resin/fiber laminae system of type AS4/3506-1. The elastic moduli of this material are listed in Table 2 according to several sources [3, 55–57].

Clearly, what is considered to be a set of material constants varies widely as it really depends on the fiber volume fraction, the fiber coating, the manufacturing process of the fiber, resin and composite and the quality of the experimental procedure overall. As can be seen from the bottom of the entries of the table where we added some statistical observations, % deviation observed varies from 11.1 % to 78.2 %. It is therefore important to identify the set of elastic material properties before and after a batch of new material is manufactured or before a material system is used for design, material qualification or material certification. To demonstrate the usage of the SSF in conjunction with design optimization we present here an example of using real data form a multiaxially loaded specimen from a test conducted by utilizing NRL66.3. The model characteristics of the specimen used are presented in Fig. 4 where in Fig. 4(a) the discretization model and potential boundary conditions are depicted, and in Fig. 4(b), a detail at the area of the left notch shows a stacking of [+60,-60]16 with each lamina made out of AS4/3506-1.

Two objective functions were constructed. Both utilized the fact that through the REMDIS-3D software, developed by our group, one can obtain full field measurements of the displacement and strain fields over any deformable body [14, 23–28].

TABLE 2: Engineering properties of AS4/3506-1 laminae

Ref.	E_{11} [GPa]	E_{22} [GPa]	E_{33}[GPa]	ν_{12}	ν_{23}	ν_{13}	G_{12}[GPa]	G_{23}[GPa]	G_{13}[GPa]
[3]	147.0	10.3	10.3	0.27	0.28	0.27	7.0	4.04	7.0
[55]	142.0	9.8	9.8	0.30	0.34	0.30	6.0	3.77	6.0
[56]	135.0	9.0	9.0	0.28		0.28	6.9		6.9
[57]	138.0	9.7	9.7	0.30	0.49	0.30	5.24	3.24	5.24
[58]	139.3	11.1	11.1	0.30	0.40	0.30	6.0	3.964	6.0
[59]	150.0	8.0	8.0	0.30		0.30	5.0		5.0
[60]	147.0	10.3	10.3	0.27		0.27	6.89		6.89
[61]	142.0	10.3	10.3	0.27		0.27	7.2		7.2
Min	135.0	8.0	8.0	0.27	0.28	0.27	5.0	3.24	5.0
Avg.	142.5	9.8	9.8	0.29	0.30	0.29	6.279	3.753	6.279
Max.	150.0	11.1	11.1	0.30	0.49	0.30	7.2	4.039	7.2
Deviation [%]	11.1	38.8	38.8	11.1	78.2	11.1	44.0	24.7	44.0
Avg. Cons.	142.5	9.81	9.81	0.29	0.30	0.29	6.279	3.769	6.279

TABLE 3: Engineering properties of AS4/3506-1 laminae

Ref	E_{11}[GPa]	E_{22} [GPa]	ν_{12}	ν_{23}	G_{12}[GPa]
Daniels [3]	147.0	10.3	0.27	0.28	7.0
Present	125.0	10.8	0.27	0.32	7.96

Thus, our experimental measurements for the formation of the objective functions were chosen to be the strains at the nodal points of the discretization shown Fig. 4(a). The first objective function chosen was based entirely on strains and is given by

$$J^{\varepsilon} = \sum_{k=1}^{N} \left(\sum_{i=1}^{2} \sum_{j=i}^{2} \left(\left[\varepsilon_{ij}^{\exp} \right]_k - \left[\varepsilon_{ij}^{fem} \right]_k \right) \right)^2 , \tag{28}$$

the second objective function is given in terms of surface strain energy density according to

$$J^U \approx \oint_{\partial\Omega} \left(U^{\exp} - U^{fem} \right)^2 dS \approx$$
$$\approx \oint_{\partial\Omega} \left(\sum_{i=1}^{2} \sum_{j=i}^{2} \sum_{m=1}^{2} \sum_{n=m}^{2} \left(s_{ijmn} \varepsilon_{ij}^{\exp} \varepsilon_{mn}^{\exp} - s_{ijmn} \varepsilon_{ij}^{fem} \varepsilon_{mn}^{fem} \right) \right)^2 dS \tag{29}$$

where $\left[\varepsilon_{ij}^{\exp} \right]_k, \left[\varepsilon_{ij}^{fem} \right]_k$ are the experimentally determined and the FEM produced components of strain are at node k. The quantities $U^{\exp}, U^{fem}$ are the surface strain energy densities formulated by using the experimental strains and the FEM produced strains respectively. An implementation of both objective functions was applied by utilizing an implementation of the DIRECT global optimizer [62], which is available within Matlab [63], and a custom developed Monte-Carlo optimizer, also implemented in Matlab. The loading conditions applied for the moveable edge of the specimen were $u_x = 0[m], u_y = 0.0005[m], u_z = 0.001[m], r_x = 0[rad], r_y = 0[rad], r_z = 0[rad]$. In Fig.5 we can see the experimentally acquired distribution of ε_{yy} (left) and the corresponding distribution produced from FEM analysis for the five identified unique elastic constants, which are shown in Table 3, in comparison to those of [3].

For the case of the FSF a two stage optimization was performed. In the first stage we determined the values of the coefficients of the strain invariant monomials in Eq. 24 such that the FSF matches the SSF by constructing and minimizing an objective function of the form

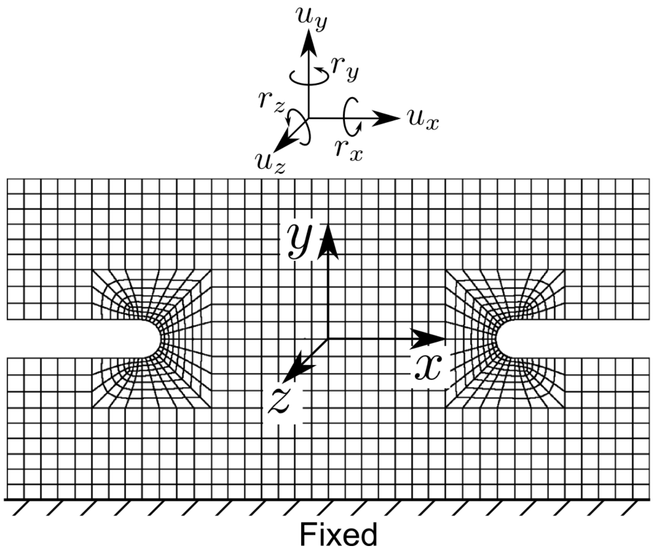

(a) Discretization and boundary conditions of typical specimen used for material characterization

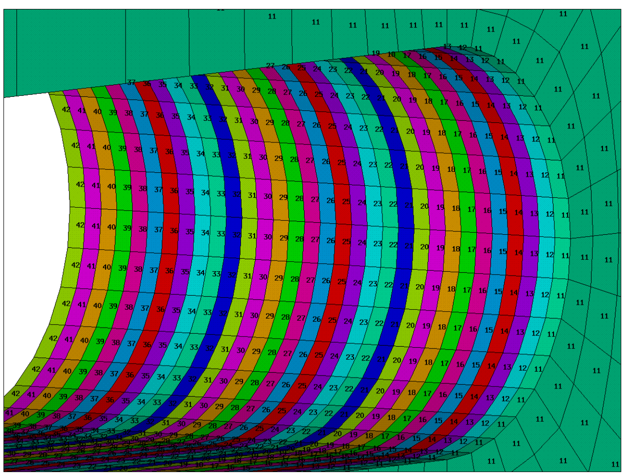

(b) Detail of FEA model near one of the notches

FIGURE 4: Finite Elements Model

$$J^{URF}(d,a_1,b_1,c_1,d_1) \approx \oint_{\partial\Omega} \left(U^R_{FSF} - U^R_{SSF}\right)^2 dS \approx$$
$$\approx \left[\oint_{\partial\Omega} \left(\sum_{i=1}^{2}\sum_{j=i}^{2}\sum_{m=1}^{2}\sum_{n=m}^{2} \left(U^R_{FSF} - U^R_{SSF}\right)\right)^2 dS\right] \tag{30}$$

This was done is order to establish the proper parameters of the FSF model that match the SSF model.

In the second stage the material parameters encoding the damage behavior of the FSF were determined through the minimization of the objective function

$$J^{UF}(d,a_1,b_1,c_1,d_1,d_a^\infty,\eta_a) \approx \oint_{\partial\Omega} \left(U^1_{FSF} - U^2_{FSF}\right)^2 dS \approx$$
$$\approx \left[\oint_{\partial\Omega} \left(\sum_{i=1}^{2}\sum_{j=i}^{2}\sum_{m=1}^{2}\sum_{n=m}^{2} \left(U^1_{FSF} - U^2_{FSF}\right)\right)^2 dS\right] \tag{31}$$

where $U^1_{FSF}(\bar{d},\bar{a}_1,\bar{b}_1,\bar{c}_1,\bar{d}_1,\bar{d}_a^\infty,\bar{\eta}_a)$ is the SED of the FSF for the parameters $\bar{d},\bar{a}_1,\bar{b}_1,\bar{c}_1,\bar{d}_1$ computed from the previous step of matching the FSF with the SSF. The parameters $\bar{d}_a^\infty,\bar{\eta}_a$ were chosen arbitrarily to be some values that can capture nonlinearity due to damage. This complete set of parameters represents the known target model of the material as shown in the second row of Table 4. The unknown constitutive model was chosen to be represented by another FSF SED, namely $U^1_{FSF}(d,a_1,b_1,c_1,d_1,d_a^\infty,\eta_a)$. The bottom row of Table 4 shows the parameters determined by minimizing the objective function in Eq. 31 via a Monte-Carlo global optimizer.

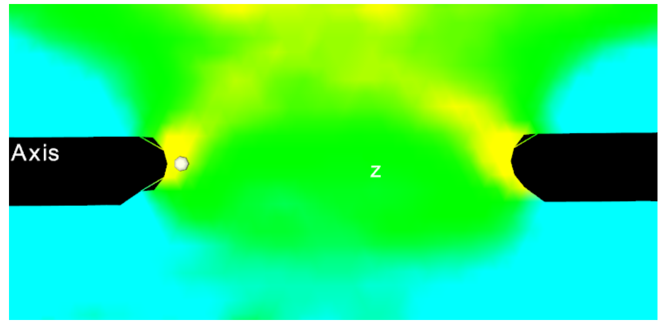

(a) Determined experimentally via MRGM

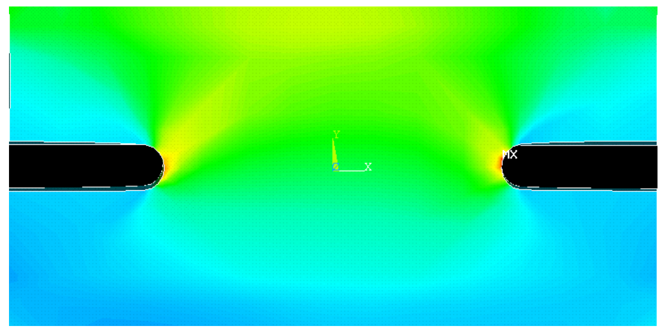

(b) Corresponding matched distribution of the numerical model as it was produced by FEA

FIGURE 5: Distributions of the vertical component of strain (ε_{yy}) for the purpose of determining the five elastic constants of AS4/3506-1 composite lamina material

TABLE 4: FSF parameters of AS4/3506-1 laminae with damage

Model	d	a_1	b_1	c_1	e_1	d_a^∞	η_a
Target	0.00007012	1611	713	29212	-458.7	0.9	1.8
Identified	0.00006987	1613	721	29105	-449.3	0.92	1.979

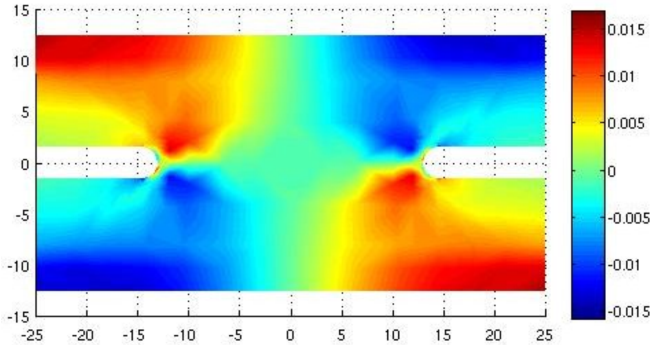

(a) Small strain formulation FEA results

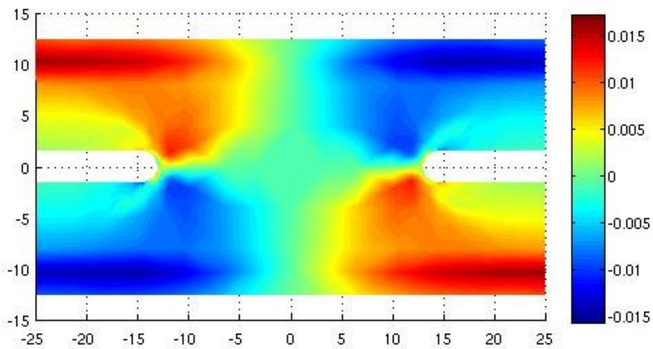

(b) Finite strain formulation FEA results

FIGURE 6: FEA results of the vertical component of strain (ε_{yy}) for the case of a specimen loaded both in tension and torsion

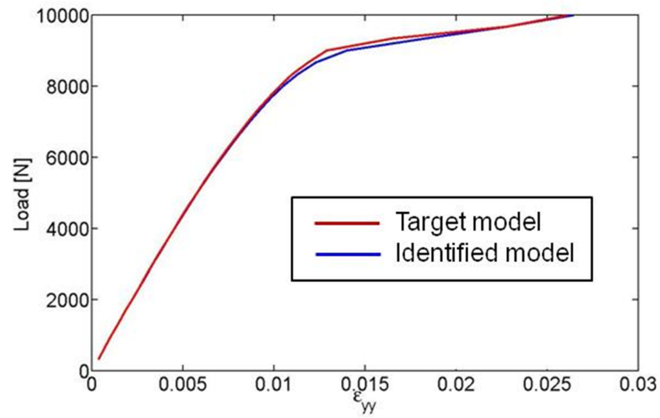

FIGURE 7: Comparison of the load vs. vertical component of strain (ε_{yy}) at a point in front of the notch, between the target and the identified model by using the FSF

An indication of how well the FSF can capture the SSF, for the case of the recoverable (linear elastic) regime, is shown in Fig. 6, where the distribution of ε_{yy} is shown for both models for a case of combined torsion and tension of the specimen. In addition, a comparison of load vs. strain evolution, for a point in front of the first of two notches, is shown in Fig. 7.

CONCLUSIONS AND DISCUSSION

We have demonstrated the application of design optimization methodologies for the determination of the constitutive response of composite materials with or without damage. Strain energy density and full field strain based approaches have been utilized to incorporate massive full field strain measurements from specimens loaded by a multiaxial custom-made loading machine. We have formulated objective functions expressing the difference between the experimentally observed behavior of composite materials under various loading conditions, and the simulated behavior via FEA, which are formulated in terms of strain energy density functions of a particular structure under identical loading conditions.

Two formalisms involving small strains and finite strains have been utilized in a manner that involves both additive decomposition of recoverable and irrecoverable strain energy density. This was done in order to address both the elastic and inelastic response of composite materials due to damage. The finite strain formulation further involves a volumetric and distortional energy decomposition.

Demonstrations have been given in terms of numerical examples utilizing both synthetic and actual data in determining both the elastic and inelastic material parameters.

We are currently working in extending these energy formulations to approaches that achieve two main goals. First, that those approaches do not require FEA in the loop and second, that they incorporate the stochastic nature of the material response and the acquired data in a manner that quantifies uncertainty.

This quantification should utilize prior knowledge via Bayesian based stochastic formalisms, which enable incremental and recursive algorithms based on Kalman filtering and in general, information theory.

ACKNOWLEDGMENT

The authors acknowledge the support by the Office of Naval Research, and by NRL's 6.1 core-program.

REFERENCES

[1] Kaczmar, J. W., Pietrzak, K., and Wlosinski, W., 2000. "The production and application of metal matrix composite materials". *Journal of Materials Processing Technology,* ***106***(1-3), pp. 58 – 67.

[2] Baker, A., Dutton, S., and Kelly, D., 2004. *Composite Materials for Aircraft Structures, Second Edition*, 2nd ed. AIAA, Oct.

[3] Daniel, I. M., and Ishai, O., 2005. *Engineering Mechanics of Composite Materials*, 2nd ed. Oxford University Press, USA, July.

[4] Carlsson, L., Adams, D. F., and Pipes, R. B., 1986. *Experimental Characterization of Advanced Composite Materials, Third Edition*, 3 ed. CRC Press, Dec.

[5] Mast, P., Beaubien, L., Clifford, M., Mulville, D., Sutton, S., Thomas, R., Tirosh, J., and Wolock, I., 1983. "A semi-automated in-plane loader for materials testing". *Experimental Mechanics,* ***23***, pp. 236–241. 10.1007/BF02320415.

[6] Mast, P. W., Nash, G. E., Michopoulos, J. G., Thomas, R. W., Badaliance, R., and Wolock, I., 1992. Experimental determination of dissipated energy density as a measure of strain-induced damage in composites. Tech. Rep. Tec. Rpt. NRL/FR/6383–92-9369, Naval Research Laboratory, Washington, DC, USA.

[7] Mast, P., Nash, G., Michopoulos, J., Thomas, R., Wolock, I., and Badaliance, R., 1995. "Characterization of strain-induced damage in composites based on the dissipated energy density Part I. Basic scheme and formulation". *Theoretical and Applied Fracture Mechanics,* ***22***(2), pp. 71–96.

[8] Michopoulos, J., 2003. *Recent advances in Composite Materials: In Honor Of S.A. Paipetis*. Kluwer Academic Press, ch. Computational and Mechatronic Automation of Multiphysics Research for Structural and Material Systems, pp. 9–21.

[9] Michopoulos, J., 2004. "Mechatronically automated characterization of material constitutive respone". In Proceedings of the 6th World Congress on Computational Mechanics (WCCM-VI), Tsinghua University Press and Springer, pp. 486–491.

[10] Michopoulos, J., Hermanson, J., and Furukawa, T., 2008. "Towards the robotic characterization of the constitutive response of composite materials". *Composite Structures,* ***86***(1-3), pp. 154–164.

[11] Pierron, F., Vert, G., Burguete, R., Avril, S., Rotinat, R., and Wisnom, M. R., 2007. "Identification of the orthotropic elastic stiffnesses of composites with the virtual fields method: Sensitivity study and experimental validation". *Strain,* ***43***(3), pp. 250–259.

[12] Cooreman, S., Lecompte, D., Sol, H., Vantomme, J., and Debruyne, D., 2007. "Elasto-plastic material parameter identification by inverse methods: Calculation of the sensitivity matrix". *International Journal of Solids and Structures,* ***44***(13), pp. 4329 – 4341.

[13] Furukawa, T., and Michopoulos, J., 2008. "Computational design of multiaxial tests for anisotropic material characterization". *International Journal for Numerical Methods in Engineering,* ***74***(12), pp. 1872–1895.

[14] Michopoulos, J. G., Iliopoulos, A. P., and Furukawa, T., 2009. "Accuracy of inverse composite laminate characterization via the mesh free random grid method". *ASME Conference Proceedings,* ***2009***(48999), pp. 367–374.

[15] Bruno, L., Furgiuele, F. M., Pagnotta, L., and Poggialini, A., 2002. "A full-field approach for the elastic characterization of anisotropic materials". *Optics and Lasers in Engineering,* ***37***(4), pp. 417 – 431.

[16] Schmidt, T., Tyson, J., and Galanulis, K., 2003. "Full–field dynamic displacement and strain measurement using advanced 3d image correlation photogrammetry: Part 1". *Experimental Techniques,* ***27***(3), pp. 47–50.

[17] Kajberg, J., and Lindkvist, G., 2004. "Characterisation of materials subjected to large strains by inverse modelling based on in-plane displacement fields". *International Journal of Solids and Structures,* ***41***(13), pp. 3439 – 3459.

[18] Meuwissen, M. H. H., Oomens, C. W. J., Baaijens, F. P. T., Petterson, R., and Janssen, J. D., 1998. "Determination of the elasto-plastic properties of aluminium using a mixed numerical-experimental method". *Journal of Materials Processing Technology,* ***75***(1-3), pp. 204 – 211.

[19] Molimard, J., Le Riche, R., Vautrin, A., and Lee, J., 2005. "Identification of the four orthotropic plate stiffnesses using a single open-hole tensile test". *Experimental Mechanics,* ***45***, pp. 404–411. 10.1007/BF02427987.

[20] Grediac, M., Toussaint, E., and Pierron, F., 2002. "Special virtual fields for the direct determination of material parameters with the virtual fields method. 1–principle and definition". *International Journal of Solids and Structures,* ***39***(10), pp. 2691 – 2705.

[21] Grediac, M., and Pierron, F., 2006. "Applying the virtual fields method to the identification of elasto-plastic constitutive parameters". *International Journal of Plasticity,* ***22***(4), pp. 602 – 627.

[22] Chalal, H., Avril, S., Pierron, F., and Meraghni, F., 2006.

"Experimental identification of a nonlinear model for composites using the grid technique coupled to the virtual fields method". *Composites Part A: Applied Science and Manufacturing,* ***37***(2), pp. 315 – 325. CompTest 2004.
[23] Michopoulos, J. G., and Iliopoulos, A. P., 2009. "A computational workbench for remote full field 2d displacement and strain measurements". *ASME Conference Proceedings,* ***2009***(48999), pp. 55–63.
[24] Andrianopoulos, N. P., and Iliopoulos, A. P., 2006. "Displacements measurement in irregularly bounded plates using mesh free methods". In Proc. 16th European Conference of Fracture, Alexandroupolis, Greece, July 3–7.
[25] Iliopoulos, A. P., Michopoulos, J. G., and Andrianopoulos, N. P., 2008. "Performance sensitivity analysis of the Mesh-Free Random Grid method for whole field strain measurements". *ASME Conference Proceedings,* ***2008***(43277), pp. 545–555.
[26] Iliopoulos, A. P., Michopoulos, J. G., and Andrianopoulos, N. P., 2010. "Performance analysis of the Mesh-Free Random Grid Method for full-field synthetic strain measurements". *Strain*, p. In Print.
[27] Iliopoulos, A., and Michopoulos, J., 27–31 Jul 2009. "Sensitivity analysis of the mesh-free random grid method for measuring deformation fields on composites". In Proceedings of the 17th International Conference on Composite Materials, ICCM-17, The British Composites Society: Edinburgh International Convention Centre (EICC), Edinburgh, UK, 2009.
[28] Iliopoulos, A. P., and Michopoulos, J. G., 2009. "Effects of anisotropy on the performance sensitivity of the Mesh-Free random grid method for whole field strain measurement". *ASME Conference Proceedings,* ***2009***(48999), Jan., pp. 65–74.
[29] Michopoulos, J. G., Hermanson, J. C., and Iliopoulos, A., 2010. "Towards a recursive hexapod for the multidimensional mechanical testing of composites". In Proceedings of the ASME 2010 International Design Engineering Technical Conferences & Computers and Information in Engineering Conference IDETC/CIE 2010, no. DETC2010/CIE-28699.
[30] Michopoulos, J., and Furukawa, T., 2007. "Multi-level coupling of dynamic data-driven experimentation with material identification". *Lecture Notes in Computer Science (including subseries Lecture Notes in Artificial Intelligence and Lecture Notes in Bioinformatics),* ***4487 LNCS***, pp. 1180–1188.
[31] Furukawa, T., Michopoulos, J., and Kelly, D., 2008. "Elastic characterization of laminated composites based on multiaxial tests". *Composite Structures,* ***86***(1-3), pp. 269–278.
[32] Man, H., Furukawa, T., and Kellermann, D., 2008. "Implicit constitutive modeling based on the energy principles". In Proceedings of XXII ICTAM, 25-59 August 2008, Adelaide 2008.
[33] Furukawa, T., and Michopoulos, J., 2008. "Online planning of multiaxial loading paths for elastic material identification". *Computer Methods in Applied Mechanics and Engineering,* ***197***(9-12), pp. 885–901.
[34] Michopoulos, J., Furukawa, T., and Lambrakos, S., 2009. "Data-driven characterization of composites based on virtual deterministic and noisy multiaxial data". In 2008 ASME International Design Engineering Technical Conferences and Computers and Information in Engineering Conference, DETC 2008, Vol. 3, pp. 1095–1106.
[35] Furukawa, T., and Pan, J. W., 2010. "Stochastic identification of elastic constants for anisotropic materials". *International Journal for Numerical Methods in Engineering,* ***81***(4), pp. 429–452.
[36] Samarasinghe, S., 2006. *Neural Networks for Applied Sciences and Engineering: From Fundamentals to Complex Pattern Recognition*, 1 ed. Auerbach Publications, Sept.
[37] Michopoulos, J., 1992. Constitutive characterization of composites via artificial neural nets. Tech. rep., Code 6383 Internal Branch Report, NRL, April.
[38] Leighton, R., 1994. Aspirin/migraines, v7.0.
[39] Yagawa, G., Yoshimura, S., Okuda, H., and Furukawa, T., 1996. *Localized Damage IV: Computer-Aided Assessment and Control*. ch. Innovative approaches for modelling of inelastic material behaviors (applications of neural networks and evolutionary algorithms), pp. 169–184.
[40] Furukawa, T., and Yagawa, G., 1998. "Implicit constitutive modelling for viscoplasticity using neural networks". *International Journal for Numerical Methods in Engineering,* ***43***(2), pp. 195–219.
[41] Furukawa, T., and Hoffman, M., 2004. "Accurate cyclic plastic analysis using a neural network material model". *Engineering Analysis with Boundary Elements,* ***28***(3), pp. 195 – 204. Inverse Problems.
[42] Man, H., Furukawa, T., Hoffman, M., Imlao, S., and Lou, Z. H., 2007. "An indirect implicit model for frequency dependent hystereses of piezoelectric ceramics". *Journal of the Australian Ceramics Society,* ***43***(2), pp. 169–174.
[43] Man, H., Furukawa, T., Hoffman, M., and Imlao, S., 2008. "An indirect implicit technique for modelling piezoelectric ceramics". *Computational Materials Science,* ***43***(4), pp. 629 – 640.
[44] Ghaboussi, J., and Sidarta, D., 1998. "New nested adaptive neural networks (NANN) for constitutive modeling". *Computers and Geotechnics,* ***22***(1), pp. 29 – 52.
[45] Shin, H. S., and Pande, G. N., 2003. "Identification of elastic constants for orthotropic materials from a structural test". *Computers and Geotechnics,* ***30***(7), pp. 571 – 577.
[46] Jung, S., and Ghaboussi, J., 2006. "Neural network constitutive model for rate-dependent materials". *Comput. Struct.,* ***84***, June, pp. 955–963.

[47] Haj-Ali, R., and Kim, H.-K., 2007. "Nonlinear constitutive models for FRP composites using artificial neural networks". *Mechanics of Materials,* ***39***(12), pp. 1035 – 1042.

[48] Man, H., Furukawa, T., Herszberg, I., and Prusty, G., 18-21 May 2009, Baltimore, MD 2009. "Implicit modeling of damage behavior for composite materials using an energy-based method". In SAMPE '09 Spring Symposium Conference Proceedings, p. 54(Paper ID: 5704).

[49] Man, H., Furukawa, T., Pan, J., Iliopoulos, A., Michopoulos, J. G., Orifici, A., and Hermanson, J. "Experimentally validated neural network constitutive modelling using energy-based characterisation". *submitted*.

[50] Matzenmiller, A., Lubliner, J., and Taylor, R. L., 1995. "A constitutive model for anisotropic damage in fiber-composites". *Mechanics of Materials,* ***20***(2), pp. 125 – 152.

[51] Haupt, P., 2002. *Continuum Mechanics and Theory of Materials*, 2nd ed. Springer, Apr.

[52] Van Der Meer, F., and Sluys, L., 2009. "Continuum models for the analysis of progressive failure in composite laminates". *Journal of Composite Materials,* ***43***(20), pp. 2131–2156.

[53] Ju, J. W., Chaboche, J., and Voyiadjis, G. Z., 1998. *Damage Mechanics in Engineering Materials*, 1st ed. Elsevier Science, Jan.

[54] Kaliske, M., 2000. "A formulation of elasticity and viscoelasticiy for fibre reinforced material at small and finite strains". *Comput. Meth. Appl. Mech. Eng.,* ***185***, pp. 225–243.

[55] Ryan, K. F. Dynamic response of graphite/epoxy plates subjected to impact loading. http://dspace.mit.edu/handle/1721.1/42982. Thesis (M.S.)–Massachusetts Institute of Technology, Dept. of Aeronautics and Astronautics, 1990.

[56] Wegner, P. M., and Adams, D. F., 2000. Verification of the combined load compression (CLC) test methods. Tech. Rep. DOT/FAA/AR-00/26, DOT/FAA.

[57] Vaidya, R., and Sun, C., 1997. "Fracture criterion for notched thin composite laminates". *AIAA J.,* ***35***(2), pp. 311–316.

[58] Minguet, P. J., Dugundji, J., and Lagace, P., 1989. "Postbuckling behavior of laminated plates using a direct energy-minimization technique". *AIAA Journal,* ***27***(12), pp. 1785–1792.

[59] Lessard, L. B., Eilers, O. P., and Shokrieh, M. M., 1995. "Testing of in-plane shear properties under fatigue loading". *Journal of reinforced plastics and composites,* ***14***(9), pp. 965–987.

[60] Esp, B., and Chan, W., 2008. "Two parameter approximation to the orthotropic stress concentration factor". In SAMPE 2008 - Long Beach, CA May 18 - 22.

[61] Bing, Q., and Sun, C., 2005. "Modeling and testing strain rate-dependent compressive strength of carbon/epoxy composites". *Composites Science and Technology,* ***65***(15-16), pp. 2481 – 2491. 20th Anniversary Special Issue.

[62] Jones, D. R., Perttunen, C. D., and Stuckman, B. E., 1993. "Lipschitzian optimization without the Lipschitz constant". *J. Optim. Theory Appl.,* ***79***(1), pp. 157–181.

[63] The Mathworks. Matlab. http://www.mathworks.com.